

Periodic X-ray modulations in Supersoft X-ray Sources¹

A Odendaal¹, PJ Meintjes¹, PA Charles² and AF Rajoelimanana^{3,4}

¹Department of Physics, University of the Free State, P.O. Box 339, Bloemfontein, 9300, South Africa

²School of Physics and Astronomy, Southampton University, Southampton SO17 1BJ

³South African Astronomical Observatory, P.O. Box 9, Observatory, 7935, South Africa

⁴Astrophysics, Cosmology and Gravity Centre (ACGC), University of Cape Town, Private Bag X3, Rondebosch, 7701, South Africa

E-mail: WinkA@ufs.ac.za

Abstract. The supersoft source CAL 83 is often considered to be the prototype of its class. We report the discovery of modulations at a period of ~ 67 s in *XMM-Newton* X-ray data of CAL 83. This may be the spin period of a highly spun-up white dwarf, which is to be further investigated with follow-up observations in both the X-ray and optical wavebands. The supersoft source SMC 13 has an orbital period of ~ 4.1 h. SMC 13 was reported in the literature to exhibit orbital modulation in its X-ray flux, as inferred from its folded *ROSAT* light curve. We report the confirmation of this orbital modulation from three *Chandra* data sets, each providing continuous coverage of ~ 2.7 complete orbital cycles.

1. Introduction

Supersoft X-ray sources (SSS) form a highly luminous ($\sim 10^{36}$ - 10^{38} erg s⁻¹) class of objects that emit more than $\sim 90\%$ of their energy below 0.5 keV. SSS were first observed with the *Einstein X-ray Observatory* (Long et al. 1981, Seward and Mitchell 1981) and further discoveries by *ROSAT* established them as a distinct class of objects (Trümper et al. 1991). Typical effective temperatures range between ~ 15 -80 eV (see Kahabka and van den Heuvel (2006) for a recent review on SSS).

It was shown by van den Heuvel et al. (1992) that the low effective temperatures and high luminosities of these sources can be explained by the nuclear burning of hydrogen on the surface of a white dwarf accreting material on the thermal time scale of the donor. The accretion rate required for steady nuclear burning is $\sim 10^{-7} M_{\odot}$ yr⁻¹, which can be sustained if the donor mass is comparable to or greater than the white dwarf mass (Paczynski 1971, Savonije 1983). Many SSS are also believed to contain accretion discs.

Recent analysis of archived data of the binary supersoft sources CAL 83 and SMC 13 showed strong modulations in the X-ray waveband. We report preliminary results of the timing analysis performed on these data, based on the results obtained during the M.Sc. research of Odendaal (2012).

¹ Based on observations obtained with *XMM-Newton*, an ESA science mission with instruments and contributions directly funded by ESA Member States and NASA, as well as observations from the *Chandra Data Archive*.

2. CAL 83 in the Large Magellanic Cloud

2.1. Observations and data calibration

CAL 83 has been observed by *XMM-Newton* several times from April 2000 to May 2009. The X-ray data were recorded with the three EPIC detectors (MOS1, MOS2 and PN) and the RGS. The data sets were calibrated by following standard data reduction procedures with the *XMM-Newton* Science Analysis System², Version 11.0. The arrival times in the event files were corrected to the solar system barycentre (TDB system). From each calibrated event file, a light curve with a binning of 10 s was created from the source photons in the 0.15-2.5 keV range.

2.2. Timing analysis

Each of the CAL 83 X-ray light curves were detrended by subtracting the mean and dividing by the standard deviation. The task SCARGLE in the Starlink PERIOD package³ was subsequently utilized to create a Lomb-Scargle (LS) periodogram from each detrended light curve (Scargle 1982).

A power peak at a $\gtrsim 2\sigma$ level near 15 mHz ($P \sim 67$ s) was found in the EPIC PN (the most sensitive of the 5 detectors) periodograms of 6 of the observations. These periodograms are shown in figure 1. The EPIC MOS periodograms of some of these observations have a very weak feature near ~ 67 s. The periodicity was not detected in the RGS periodograms.

The EPIC PN data of the 6 data sets exhibiting the periodicity were reanalysed by subdividing the longer data sets into shorter light curves and creating a similar LS periodogram for each. The results from the segments exhibiting the periodicity are summarized in table 1. The error bars on the period values were determined by the intrinsic Fourier resolution of each periodogram, which gives an error of $P^2/2T$ to each side of each period peak, where P is the period, and T the total length of the light curve.

It is evident from table 1 that the detected period varies over a range of several seconds. The power of the peak is also highly variable for the different periodograms. No obvious correlation was found between the mean count rate and peak power, although it was noted that the period was not detected in data sets where the EPIC PN count rate was below 1 count/s.

2.3. Discussion

The exact origin of the ~ 67 s period is still under investigation. As the periodicity was found in the X-ray data, it is associated with the white dwarf. The fact that the modulation at ~ 67 s is present in different data sets spanning over about 9 years possibly rules out short-lived quasi-periodic oscillations. A very promising possibility is that the periodicity represents the spin period of a magnetized white dwarf in CAL 83. The period is reminiscent of the short white

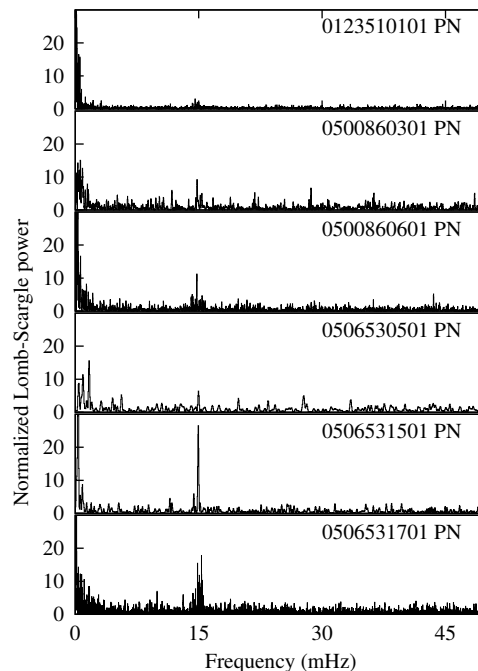


Figure 1. LS periodograms of EPIC PN observations exhibiting ~ 67 s periodicity.

² <http://xmm.esa.int/sas/>

³ <http://www.starlink.rl.ac.uk/star/docs/sun167.htx/sun167.html>

Table 1. Timing analysis of the CAL 83 *XMM-Newton* PN light curves exhibiting a ~ 67 s periodicity. “Peak power” refers to normalized power from Lomb-Scargle periodogram.

Obs ID	Length (s)	BJD (middle)	Period (s)	Peak power	Mean PN counts/s	Principal investigator
0123510101	5000	2451657.95459	68.6 ± 0.5	7.8	7.3	Fred Jansen
	5000	2451658.06917	67.9 ± 0.5	9.8	5.9	
	5000	2451658.12704	67.2 ± 0.5	5.2	6.7	
	5000	2451658.24162	67.2 ± 0.5	12.5	3.4	
	5000	2451658.29949	66.3 ± 0.4	7.7	3.0	
0500860301	5240	2454288.51696	65.0 ± 0.4	7.8	6.9	Thierry Lanz
	5240	2454288.57761	67.5 ± 0.4	8.6	6.8	
0500860601	5010	2454429.44780	67.8 ± 0.5	5.1	5.9	Robert Schwarz
	5010	2454429.56378	67.8 ± 0.5	9.3	6.9	
	5010	2454429.62176	69.9 ± 0.5	10.6	7.2	
0506530501	4600	2454573.12196	66.8 ± 0.5	6.6	2.1	Robert Schwarz
0506531501	6480	2454691.16206	66.9 ± 0.3	27.6	9.3	
0506531701	4570	2454981.86631	67.6 ± 0.5	7.8	8.8	
	4570	2454981.91920	66.6 ± 0.5	10.5	8.7	
	4570	2454981.97210	66.1 ± 0.5	15.9	9.2	
	4570	2454982.02499	64.9 ± 0.5	6.4	9.4	
	4570	2454982.07788	64.9 ± 0.5	5.5	7.9	
	4570	2454982.13078	67.3 ± 0.5	8.5	10.0	
	4570	2454982.18367	67.6 ± 0.5	4.7	9.8	
	4570	2454982.23657	66.1 ± 0.5	6.9	9.8	
	4570	2454982.28946	65.4 ± 0.5	15.6	8.9	
	4540	2454982.34224	65.3 ± 0.5	16.5	9.2	

dwarf spin periods in the cataclysmic variables AE Aqr (~ 33 s), V533 Her (63.633 s) and DQ Her (142 s) (Norton et al. 2004).

If it does represent the white dwarf spin period, one would expect the detected period to have exactly the same value in different data sets. However, it must be kept in mind that, although the arrival times have been corrected to the solar system barycentre, the orbital motion of the white dwarf will also modulate the detected spin period. This possibility is still under investigation.

Consistent modulations in other supersoft sources that have been ascribed to the spin period of a magnetized white dwarf are e.g. the 217.7 s pulsations in the source XMMU J004252.5+411540 in M31 (Trudolyubov and Priedhorsky 2008), and the 1110 s pulsations in Nova M31N 2007-12b (Pietsch et al. 2011). The recurrent nova RS Oph exhibited an unstable ~ 35 s periodicity during the supersoft phase after its 2006 outburst (see Osborne et al. (2011) and references therein). The favoured explanation of this variable modulation is the possibility of non-radial oscillations caused by nuclear burning instabilities. It may be that the ~ 67 s X-ray periodicity in CAL 83 is due to a similar effect.

3. SMC 13 in the Small Magellanic Cloud

The orbital period of SMC 13 was first reported by Schmidtke et al. (1994), but the most recent orbital ephemeris is that of van Teeseling et al. (1998) (with the number on the left denoting the time of minimum light, and the one on the right the orbital period of 0.1719260 ± 0.0000007 days):

$$T_0 = \text{HJD } 2450434.1320 \pm 0.0006 \quad + \quad 0.1719260E \pm 0.0000007 \text{ d} .$$

Kahabka (1995) reported the discovery of orbital modulation in the *ROSAT* data of SMC 13, and Kahabka (1996) determined the *ROSAT* period to be 4.123 h (0.1718 d).

Table 2. Archived *Chandra* X-ray observations of SMC 13.

Obs ID	Instrument	Start date & time (UT)	Exposure time (s)	PI
4535	ACIS-S3	2005-01-30 16:56:17	40 140	J. Greiner
7456	HRC-S+LETG	2007-02-12 18:25:16	40 190	T. Lanz
8519	HRC-S+LETG	2007-02-18 00:42:08	42 670	T. Lanz

3.1. Observations and data calibration

We discuss 3 archived *Chandra X-ray Observatory* observations of SMC 13, which are summarized in table 2. The calibration of the data was carried out by following standard data reduction and processing procedures with the CIAO software⁴, Version 4.3, using Version 4.4.5 of the CALDB (CIAO Calibration Database). The arrival times in the calibrated event files of the three observations were corrected to the solar system barycentre (TDB system).

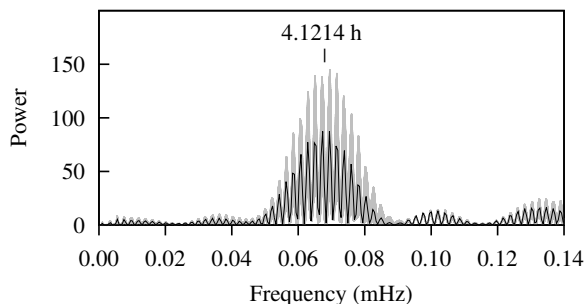
3.2. Timing analysis

The PERIOD task SCARGLE was used to search for an orbital period in the *Chandra* X-ray light curves around the period of 4.123 h found by Kahabka (1996) in the *ROSAT* data. Each of the three Lomb-Scargle periodograms exhibited a strong power peak at the approximate position of the orbital period. However, the uncertainty in the peak positions was very high due to the relatively short length of the individual data sets. Therefore the X-ray modulation could be constrained to nothing better than 4.44 ± 0.89 h with the separate observations.

To obtain a higher period resolution, two additional Lomb-Scargle periodograms were created (see figure 2 for the region around the strongest peak): one by combining all three observations, and the other by combining only the observations of February 2007 (Obs 7456 and 8519). The presence of numerous alias peaks is evident, as well as possible harmonics of the orbital period. The strongest peak in the 2007 periodogram was determined to be at a period of 4.12 ± 0.06 h. The position of this (relatively broad) peak was then used to choose the appropriate peak on the high time-resolution periodogram obtained by combining all three data sets, yielding a period of 4.1214 ± 0.0005 h. The error value was calculated with the method described in Section 2.2, considering the total time from the start of Obs 4535 to the end of Obs 8519.

The *ROSAT* light curves of Kahabka (1996) in the soft (S: 0.1-0.25 keV) and hard (H: 0.26-0.50 keV) energy bands, as well as the hardness ratio, folded on the ephemeris of Schmidtke et al. (1994) are shown in figure 3.

The intrinsic energy resolution of the ACIS-S detector was used to create two similar *Chandra* light curves: one in the soft band (S: 0.100-0.250 keV) and one in the hard band (H: 0.251-0.500 keV). For both the *ROSAT* and the *Chandra* light curves, the hardness ratio was calculated as $HR=(H-S)/(H+S)$. The soft, hard and HR light curves of observation 4535 were folded on the newly determined period by making use of the task **efold** in the Xronos Timing Analysis Software Package⁵, using the time of minimum light of the third minimum of the Obs 4535 light curve (BJD 2453401.5682), and these are provided in figure 4.

**Figure 2.** Lomb-Scargle periodograms of combined SMC 13 *Chandra* light curves. Black: Obs 7456 and 8519. Gray: Obs 4535, 7456 and 8519.

⁴ <http://cxc.harvard.edu/ciao/index.html>

⁵ See the Xronos User's Guide (HEASARC 2009) for more information.

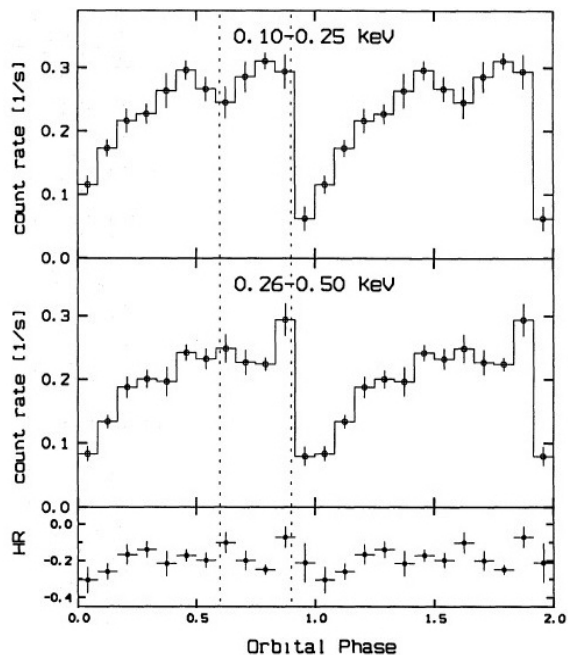


Figure 3. *ROSAT* light curves of SMC 13, folded on 4.123 h with respect to the epoch Nov. 3.105, 1994. (Adopted from Kahabka (1996, figure 3).)

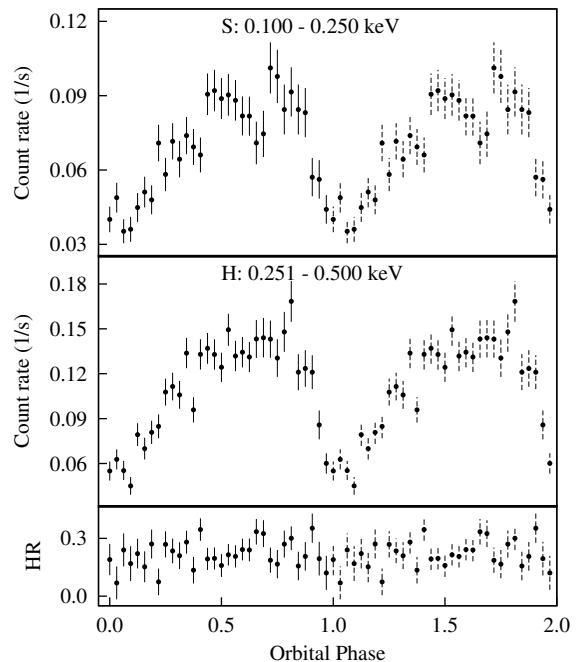


Figure 4. *Chandra* ACIS light curves of SMC 13, folded on $P_{\text{orb}} = 4.1214$ h with respect to the third minimum in the data set.

3.3. Discussion

Because the time of minimum in the *ROSAT* light curve is largely defined by only three data points, Crampton et al. (1997) mentioned the possibility that these few minima might be caused by the system being in a low state at some epochs, rather than by orbital modulation. However, each of the *Chandra* data sets constitutes an uninterrupted observation of the source for a duration of ~ 2.7 full orbital periods, and the orbital modulation is clearly evident.

The orbital period of 4.1214 ± 0.0005 h determined from the combined data set is very close to the $P_{\text{orb}} = 4.126224 \pm 0.000017$ h determined by van Teeseling et al. (1998) from photometrical data, although not included in its error ranges. However, the aliasing effects arising from the long time gaps between the *Chandra* observations made it very difficult to choose the appropriate peak, therefore the van Teeseling et al. (1998) period is considered to be more reliable.

Comparison of the folded *ROSAT* and *Chandra* light curves in figure 3 and figure 4 shows that they exhibit the same sharp, asymmetric form. As pointed out by Kahabka (1996), there seems to be a second dip at $\phi = 0.6$ in the 0.1-0.25 keV (S) band in addition to the main minimum at $\phi \sim 0.9-1.1$ in the *ROSAT* data, which is not present in the 0.26-0.50 keV (H) band. This is also visible in the *Chandra* light curves. The large amplitude variation may be ascribed to the eclipse of the primary taking place in a high inclination system. If this is the case, the fact that the eclipse is not total indicates that there is an extended emitting region. The structure of the light curve may be the result of variable absorption in the system, possibly by an accretion disc edge. As mentioned below, Kahabka (1996) also considered the possibility of SMC 13 being a polar-like system.

The hardness ratios (HR) for the 2 detectors can not be compared directly, as the H and S counts depend on detector sensitivity. However, there does seem to be an increase in HR during the minor dip, and just before the major dip for both *ROSAT* and *Chandra*. It is also interesting to note that the count rate in the H band correlates with the variations in HR. The favoured

explanation of Kahabka (1996) for this HR modulation is that it may be due to temperature variations, as an increase in temperature would result in an increase in both the HR and the count rate. Kahabka (1996) suggested that a changing observed temperature can be explained if the white dwarf is magnetized, as this would result in a changing viewing angle of the polar caps or an accretion column at the polar caps.

From figure 3, it appears that the X-ray modulation is in phase with the orbital motion. On the other hand, Schmidtke et al. (1996) found that the X-ray minimum occurs about 0.25 of an orbital cycle earlier than the optical minimum, according to their ephemeris. However, folding the *Chandra* light curves through the orbital ephemeris of van Teeseling et al. (1998) showed that the X-ray minima approximately coincides with the optical minimum. Therefore a more in-depth analysis of the orbital period and ephemeris in conjunction with previous observations of SMC 13 needs to be carried out. In particular, simultaneous optical and X-ray observations are needed to clarify the relative phasing of the minima in these wavebands. If the minima they do not coincide, it can indicate a situation where the main sources of X-ray and optical flux respectively are not aligned and therefore not eclipsed simultaneously, for example with the X-rays being brightest close to the compact object, and an optically bright “hot spot” where the accreting stream hit an accretion disc rim.

Probing periodicities in supersoft sources can therefore be instrumental in understanding these systems. With timing analysis, orbital and spin periods and also various types of quasi-periodic signals can be detected and can provide information on the orbital parameters and component masses, as well as the nature of the compact object and accretion process.

Acknowledgments

The financial assistance of the South African Square Kilometre Array Project towards this research is hereby acknowledged. Opinions expressed and conclusions arrived at, are those of the author and are not necessarily to be attributed to the NRF. We would like to thank the principal investigators of the archived X-ray data for the opportunity to analyse the data, as well as Frank Haberl for his comments on the periodicity detected in CAL 83.

References

- Crampton D, Hutchings J B, Cowley A P and Schmidtke P C 1997 *ApJ* **489**, 903–11.
- HEASARC 2009 *Xronos: A Timing Analysis Software Package. User's Guide Version 5.22*. Available at: <http://heasarc.gsfc.nasa.gov/docs/xanadu/xronos/>.
- Kahabka P 1995 in H. Böhringer et al, ed., ‘Seventeenth Texas Symposium on Relativistic Astrophysics and Cosmology’ Vol. 759 of *Annals of the New York Academy of Sciences* p. 324.
- Kahabka P 1996 *A&A* **306**, 795–802.
- Kahabka P and van den Heuvel E P J 2006 Cambridge University Press New York chapter 11, pp. 461–74.
- Long K S, Helfand D J and Grabelsky D A 1981 *ApJ* **248**, 925–44.
- Norton A J, Wynn G A and Somerscales R V 2004 *ApJ* **614**, 349–57.
- Odendaal A 2012 A Multi-Wavelength Study of Super Soft X-ray Sources in the Magellanic Clouds Master’s thesis University of the Free State Bloemfontein.
- Osborne J P et al. 2011 *ApJ* **727**, 124–33.
- Paczyński B 1971 *ARA&A* **9**, 183–208.
- Pietsch W, Henze M, Haberl F, Hernanz M, Sala G, Hartmann D H and Della Valle M 2011 *A&A* **531**, A22.
- Savonije J 1983 in W. H. G. Lewin & E. P. J. van den Heuvel, ed., ‘Accretion-Driven Stellar X-ray Sources’ pp. 343–66.
- Scargle J D 1982 *ApJ* **263**, 835–853.
- Schmidtke P C, Cowley A P, McGrath T K, Hutchings J B and Crampton D 1994 *IAU Circulars* **6107**, 1.
- Schmidtke P C, Cowley A P, McGrath T K, Hutchings J B and Crampton D 1996 *AJ* **111**, 788–93.
- Seward F D and Mitchell M 1981 *ApJ* **243**, 736–43.
- Trudolyubov S P and Priedhorsky W C 2008 *ApJ* **676**, 1218–25.
- Trümper J et al. 1991 *Nature* **349**, 579–83.
- van den Heuvel E P J, Bhattacharya D, Nomoto K and Rappaport S A 1992 *A&A* **262**, 97–105.
- van Teeseling A, Reinsch K, Pakull M W and Beuermann K 1998 *A&A* **338**, 947–56.